⚙ Environmental Systems Research

Adsorptive removal of malachite green dye from aqueous solution onto activated carbon of *Catha edulis* stem as a low cost bio-adsorbent

Gietu Yirga Abate*🔟, Adugna Nigatu Alene, Adere Tarekegne Habte and Desiew Mekuanint Getahun

Abstract

Background: The release of hazardous synthetic dyes into industrial effluents has emerged as an environmental problem requiring remediation. The present study focused on the preparation of a new and environmentally-friendly material (adsorbent) for the remediation of hazardous dyes from aqueous solution. The low cost adsorbent was prepared from locally available khat (*Catha edulis*) stem which considered as waste and accumulated on waste disposal areas of Woldia town, Ethiopia. Comprehensive characterization studies were carried out on the bio-adsorbent such as proximate analyses, specific surface area, point of zero charge and FT-IR analysis.

Results: The proximate analysis shows the prepared adsorbent has very high fixed carbon content (83.65%), which refers to high quality of the adsorbent. The adsorption performance of the prepared activated carbon was optimized by varying operational parameters such as initial dye concentration (10 mg/L), pH (10), dosage (0.5 g), and contact time (60 min). The maximum removal efficiency of the prepared adsorbent at those optimum conditions was 98.8%. The experimental data was tested by most common kinetics and isotherm models. It was observed that the pseudo-second-order kinetic model fits better with good correlation coefficient and the equilibrium data fitted well with the Freundlich isotherm model.

Conclusion: In summery this study demonstrated that the waste bio sorbent could be employed as an effective and eco-friendly alternative for the cleanup of dye-polluted aqueous system.

Keywords: Khat (*Catha edulis*), Bio sorption, Activation, Adsorbent capacity, Green dye

Background

One of the major problems faced by many countries around the world is the increase in industrial activities releases effluents containing pollutants such as heavy metal ions, organic dyes and pharmaceuticals into the aquatic environment, which cause significant health hazards to living organisms and overall deterioration of the environment (Deng et al. 2011; Munagapati et al. 2018; Nhung et al. 2018). Among different industrial pollutants colored materials and dyes constitute the focus of many environmental concerns because of their

non-biodegradable and polluting nature (Ai et al. 2011; Bello et al. 2010; Georgin et al. 2018; Mall et al. 2005). The source of these dyes are different dye manufacturing and processing industries such as textile, paper, plastics, cosmetics, leather and food as they use dyes for coloring their products (Ai et al. 2011). Among the various industrial dyes malachite green (MG), tri-phenyl methane water soluble cationic dye, has been widely used for the dyeing of leather, wool and silk, paper, as well as in distilleries (Dos Reis et al. 2011). In addition, MG is also used as a fungicide, tropical anti-protozoal agent, and antiseptic in the aquaculture industry to control fish parasites and disease (Georgin et al. 2018; Raval et al. 2016; Yakout and Shaker 2016). However, MG is very dangerous and highly cytotoxic to mammalian cells; it also acts as a liver

*Correspondence: Geitu03@gmail.com
Department of Chemistry, Woldia University, Post Office Box, 400, Woldia, Ethiopia

tumour-enhancing agent, carcinogenic, mutagenic and teratogenic effects on human health and biota (Yakout and Shaker 2016; Zhang et al. 2014).

About 50% of the total world production of dyes goes off during the dying process and have been release in textile effluents (Sharma et al. 2010). Also, the presence of very small amounts of dyes in water < 1 ppm for some dyes is highly visible, very difficult to biodegrade, extremely difficult to eliminate in natural aquatic environments and undesirable. Moreover, most of these dyes can cause allergy, dermatitis, skin irritation and also provoke cancer and mutation in humans (Ghaedi et al. 2015; Regti et al. 2017). Hence, their removal from industrial effluents before discharge into the environment is extremely important. A number of technologies have been applied over the years for the treatment of dye-containing wastewaters such as flocculation membrane filtration, precipitation, electrochemical, and adsorption can be used successfully for the removal of different dyes and pigments from aqueous phase (Asfaram et al. 2014; Silveira et al. 2014). Each technique has its own advantages and drawbacks. The literature indicates that nowadays, those dye removal techniques and investigations are dominant through adsorption technology (Fito et al. 2019; Mezohegyi et al. 2012). The use of wasted martial as adsorbents has received especial interest from several researchers for different reasons such as high selectivity, low cost, availability, and efficiency (Giwa et al. 2013; Mezohegyi et al. 2012). According to different scholar findings the following martials were used for removal of dyes such as: agricultural wastes (Kadirvelu et al. 2003), magnetite loaded multi-wall carbon nanotube (Ai et al. 2011), treated avocado shells (Georgin et al. 2018), Brazilian pine-fruit shell (Royer et al. 2009), spent coffee (Safarik et al. 2012), montmorillonite clay (Almeida et al. 2009), Fe_3O_4 nanoparticle (Ghaedi et al. 2015), activated carbon, graphene oxide, and carbon nanotubes (Li et al. 2013), palm oil mill effluent waste (Gobi et al. 2011), Bagasse Fly Ash (Gupta et al. 2000), tree fern (Ho et al. 2005) etc. Various new materials with interesting adsorption capacities that can be used on sorption processes are discovered every year.

In Ethiopia one of the major problems in cities is the use of *Catha edulis* leaves for stimulating purpose and discarding unusable part. Khat or in its scientific name *Catha edulis*, is a dicotyledonous evergreen shrub of the family Celastraceae (Kennedy 1987). The oral traditions claim that *Catha edulis* originated from Yemen; however the literature indicates that *Catha edulis* originated from Ethiopia, specifically in Hararghe with a gradual expansion to different parts of Ethiopia, Yemen and other parts of the world. Studies on the chemical composition of the extracts of *Catha edulis* leaves identified as different

compound under the group of alkaloids, terpenoids, flavonoids, sterols, glycosides, tannins, amino acids, vitamins, and minerals (Nigatu and Libsu 2019). *Catha edulis* consumers mostly use only the tip fleshy leaf part of the plant and throw the stems away which is considered as a waste and get disposed of everywhere especially around the Khat market areas, streets, and dumpsters area in Woldia town, Ethiopia. The present study focused on the development activated carbon from khat (*Catha edulis*) stem by physical and chemical activation process for removal of basic cationic dye (malachite green dye) from aqueous solutions.
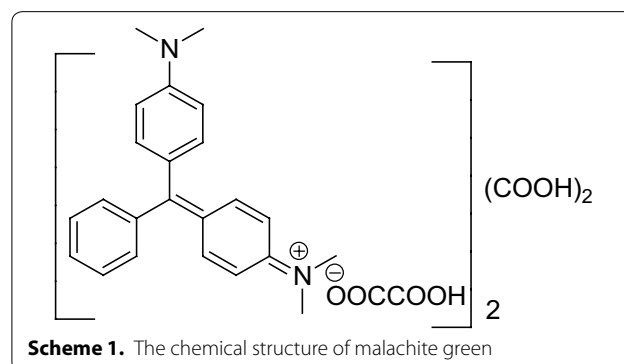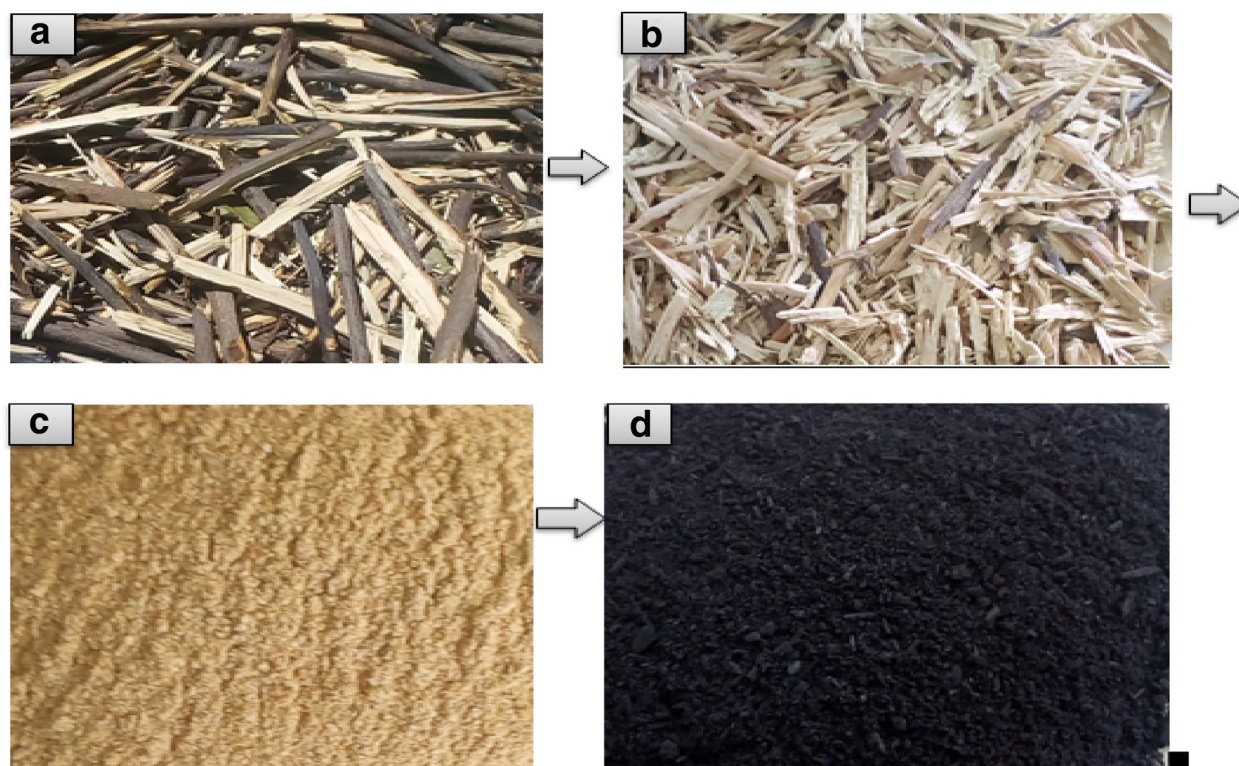
Materials and methods
Chemicals used
MG dye powder was taken from Woldia University, chemistry department laboratory and other reagents used in this work were purchased from sigma Aldrich. All the chemicals were analytical reagent grade and used as such without further purification. Malachite green oxalate [CI = 42,000, CAS number = 123333-61-9, λ_{max} = 618 nm] has a chemical formula of $C_{52}H_{54}N_4O_{12}$ with molecular weight of 927.00 g/mol. The chemical structure of MG dye is presented in Scheme 1 below.

Deionized and distilled water were used to prepare all solutions. The MG stock solution was prepared by dissolving an accurately weighed quantity of dye in deionized water and was subsequently diluted to the required concentrations. The maximum wave length was determined by scanning a known concentration of dye from 200 to 800 nm using UV–vis spectroscopy.

Adsorbent preparation
Sample preparation was conducted according to (Fito et al. 2019; Ghaedi et al. 2012, 2014; Regti et al. 2017) with little modifications and presented on Fig. 1 in short summary. Khat (*Catha edulis*) stem samples used for the preparation of activated carbon were collected from dumping sites "Khat terra" of Woldia town,

Scheme 1. The chemical structure of malachite green

Abate *et al. Environ Syst Res* (2020) 9:29

Page 3 of 13

Fig. 1 **a** Stem of khat (*Catha edulis*), **b** chopped stem of khat (*Catha edulis*), **c** powdered oven dried sample of khat (*Catha edulis*), **d** activated carbon of khat (*Catha edulis*)

Ethiopia. The sample was washed with distilled water to remove dust and any other water soluble impurities in the sample. Then the stem exposed to sunlight for several dyes and then oven dried at 105 °C until completely dried and cut into pieces at the size of 10 mm. The dried material was then milled by ball miller and separated by manually shaking stainless steel mesh screens with the opening of standard 1 mm sieve size. The sieved raw material was physically activated by carbonization in a muffle furnace (Nabertherm B180) for 2 h at 400 °C in the absence of air by placing the sample in a well-sealed stainless steel tube. Then the sample was allowed to cool for a few minute and it ready for chemical activation. The chemical activation was carried out by taking appropriate weight of powdered sample and immersed in 1 N of NaOH with a mass ratio (1:5 w/v) for 12 h. The soaked sample was filtered by Whatman filter paper and washed with 2 N of HCl several times and then with distilled water until the pH reached to neutral. The resulting activated carbon was completely dried at 110 °C in an oven for 3 h in order to achieve good carbon structure and a large surface area and kept in desiccators for further study.

Characterization of prepared adsorbent

The physicochemical properties of the adsorbent such as moisture content, ash content, volatile matter, and fixed carbon were determined according to (Bello et al. 2017; Fito et al. 2019; Temesgen et al. 2018) with slight modifications. The thermal drying method was applied for the proximate analysis of the adsorbent.

Moisture content

The adsorbent sample of 1.0 g was weighed in triplicate and placed in a clean, dried, and weighed crucible in a preheated oven at 110 °C. The crucibles with samples were placed in an oven at 110 °C for 2 h. Then, the sample was cooled in desiccators at ambient temperature and its weight was measured again. Hence, the difference between the initial (M_0) and the final mass (M_1) of the CAC was used to determine the moisture content using Eq. 1.

$$Moisture\ content\ (MC) = \frac{M_0 - M_1}{M_0} \times 100. \quad (1)$$

Ash content

About 1 g of adsorbent sample was placed in crucibles, weighted and heated in a muffle furnace (Nabertherm B180) under a temperature of 500 °C for 4 h. After that, the crucibles containing sample was allowed to cool in a desiccator to room temperature and reweighed. The ash content of sample was calculated using the Eq. 2.

$$Ash\ content\ (AC) = \frac{M_s}{M_a} \times 100; \tag{2}$$

where M_a and M_s are the mass (g) of the adsorbent and ash, respectively.

Volatile mater

For the determination of the volatile matter of the adsorbent, 1.0 g of the activated carbon sample was taken and placed in a pre-dried crucible and heated in a muffle furnace regulated at 800 °C for 8 min. Ten, the crucible was cooled in desiccators and weighed. Finally, the volatile matter of the activated carbon was calculated using Eq. 3.

$$Volatile\ matter\ (VM) = \frac{M_1 - M_2}{M_1} \times 100; \tag{3}$$

where M_1 and M_2 are initial mass (g) of adsorbents and final mass (after drying), respectively.

Fixed carbon content

It was determined by deducting the moisture, volatile, and ash content percentage from 100% using the Eq. 4.

$$Fixed\ carbon\ content\ (FC)\% = 100\% - (MC + AC + VM)\%. \tag{4}$$

Surface area determination

The specific surface area of the adsorbent was estimated according to sear method (Ahmad et al. 2013; Jawad et al. 2019). About 1.5 g prepared adsorbent was mixed with 30 g NaCl and dissolved by 100 mL of distilled water using 250 mL conical flask. The mixtures were stirred for 5 min. Then, the pH of solution was adjusted to 4, and the solution was titrated by 0.1 M NaOH until pH of the solution reaches to 9. The volumes of NaOH required to change pH value from 4 to 9 were recorded. The specific surface area of sample was obtained using the following formula:

$$specific\ surface\ area\ \left(\frac{m^2}{g}\right) = 32V - 25; \tag{5}$$

where V is the volume of 0.1 M NaOH required to raise the pH from 4.0 to 9.0. The pH point of zero charge

(pH$_{pzc}$) of the adsorbent was estimated according to (Bello and Ahmad 2012; Khan et al. 2013a; Kibami et al. 2014) with slight modifications.

Fourier transforms infrared spectroscopy (FT-IR) characterization The surface functional group of the prepared activated carbon was estimated by using FTIR spectroscopy (JASCO model 4100). The sample was mixed with dry KBr in the ratio of 2:200 in mg and ground very well. The adsorbent sample was scanned over a wavelength range of 400–4000 cm^{-1} using FTIR spectrophotometry.

Batch adsorption experiments

The adsorption experiments were carried out according to (Dos Reis et al. 2011; Ghaedi et al. 2014; Li et al. 2013, 2019) with slight modifications. The influences of experimental parameters of initial dye concentration (10–50 mg/L, step size: 10 mg/L) and pH (2–12, step size: 2) and adsorbent dose (0.2–1.4 g, step size: 0.3 g, string speed 400 rpm and at room temperature (25 °C) on the removal of MG were studied in a batch mode of operation. A measure amount of known concentration dye sample (50 mL) and 0.5 g adsorbent was taken in 250 mL of conical flask and the desired solutions pH was adjusted with 0.1 M HCl or 0.1 M NaOH for batch experiment. The mixed solutions agitated with magnetic stirrer on digital hot plate at 400 rpm until the required time reached and then the adsorbent was separated from solution by centrifugation at 4000 rpm for 10 min. The absorbance of remain supernatants solutions were determined by using UV–Vis spectrophotometer at a maximum wave length of 618 nm. The equilibrium adsorption capacity, q_e (mg/g) and removal efficiency were calculated by Eqs. 6 and 7 as follows:

$$q_e\left(\frac{mg}{g}\right) = \frac{(C_0 - C_1)V}{m}; \tag{6}$$

$$Removal\ efficiency\ (\%) = \frac{C_0 - C_1}{C_0} \times 100; \tag{7}$$

where C_0 is the initial dye concentration (mg/L); C_e is the residual concentrations of the dye (mg/L) at equilibrium; V is the volume of the dye solution (L); m is the mass of the adsorbents (g).

Kinetic studies were also followed according to the method described in batch equilibrium method above. The adsorption capacity q_t (mg/g) at different contact time t (min) was determined using the following equation:

$$q_t\left(\frac{mg}{g}\right) = \frac{(C_0 - C_t)V}{m}; \tag{8}$$

where C_0, C_e, and C_t (mg/L) are MB solution concentrations at initial, equilibrium, and time t (min), respectively. In order to determine the maximum adsorption capacity, the amount of MG adsorbed by activated carbon of *Catha edulis* based on initial MG concentration was applied to Freundlich and Langmuir isotherms.

Result and discussion
Characterization of activated carbon
Proximate analysis results
The physicochemical properties of *Catha edulis* activated carbon was determined by standard method and presented in Table 1 below. The result showed that the prepared activated carbon has very high fixed carbon content (83.65%), very low moisture content (5.38%), very low ash content (6.72%) and very low volatile matter (4.25%). This is due to carbonization and activation processes, organic substances become unstable as a result of the heat causing the molecules to break their bonds and linkages and volatile matter is released as gas and a liquid product which evaporates off leaving a material with high carbon content (Bello et al. 2017). The high composition of the fixed carbon refers to high quality of the adsorbent which improves the surface area and adsorption performance. From the result the low ash content in the activated carbon indicates inorganic matter in the sample is insignificant. According to different scholar findings high fixed carbon, low moisture, low volatile matter and low ash content adsorbents are recommendable for adsorption activities (Fito et al. 2019; Mopoung et al. 2015; Pathania et al. 2017). Therefore the prepared activated carbon is efficient as it shown by various proximate analysis.

The specific surface area of the prepared activated carbon based on sear method analysis is presented in Table 2. Based up on this result the prepared adsorbent has very high surface area, it may arise from sodium hydroxide activation. Upon high concentration sodium hydroxide activation, leads to reorganization of the chemical constituents and subsequent deposition of carbon-rich molecules to the voids of biomass by the influence of temperature and pressure increase surface

**Table 1 Proximate analysis results of the activated carbon derived from Khat (*Catha edulis*) stem**

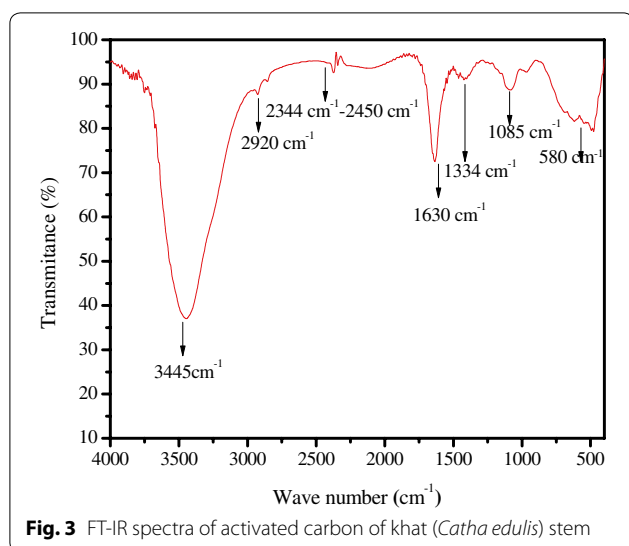| Proximate analysis	Mass in percent (%)
Moisture content	5.38
Ash content	6.72
Volatile matter	4.25
Fixed carbon	83.65

Table 2 Sear method surface area analysis

Adsorbent	Volume of sodium hydroxide consumption (mL)	Specific surface area (m²/g)
Activated carbon from *Catha edulis*	55 mL	1735 m²/g

area of the adsorbent (Deng et al. 2011; Islam et al. 2015). This results agreed with the reported value of BET analysis of activated carbon in other scholar findings (Li et al. 2013).

Determination of pH$_{pzc}$ The point of zero charge is defined as the condition in which the density of electric charge on the adsorbent surface is zero. In this study, the solid addition method was followed. Accordingly, 0.01 M (50 mL) of NaCl solution poured into 12 flasks each containing 0.1 g of adsorbent. The pH of the solutions was measured from 2 to 12 by using a pH meter and kept for 24 h. The results were then plotted between "pH final versus pH initial". The point of intersection of the curves of "pH final versus pH initial," is the PZC of adsorbent. The plot of pH final versus pH initial for both adsorbents is presented in Fig. 2. It was found to be 7.6. When the pH of the solution is below the PZC, the surface of the adsorbent will become positively charged and when the solution pH is greater than PZC, the surface of the adsorbent will become negatively charged (Temesgen et al. 2018). It implied that the prepared adsorbent was most probably adsorbing malachite green dye on basic regions.
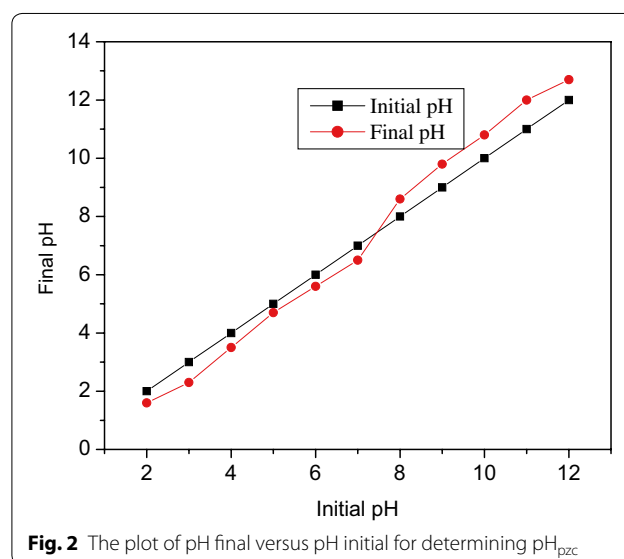
Fig. 2 The plot of pH final versus pH initial for determining pH$_{pzc}$

Abate *et al. Environ Syst Res*   (2020) 9:29

Page 6 of 13

Fig. 3 FT-IR spectra of activated carbon of khat (*Catha edulis*) stem

FTIR analysis

FT-IR analysis result of activated carbon of *khat* (*Catha edulis*) is presented in Fig. 3, below. The spectra revealed various functional groups detected on the surface of activated carbon of *khat* (*Catha edulis*). The broad band at 3440 cm^{-1} corresponded to O–H stretching of hydroxyl group. A pair of bands at 2920 and 2840 cm^{-1} could be attributed to C–H stretching of alkane group (Ahmad et al. 2017; Lee et al. 2016). The band interval from 2345 to 2450 cm^{-1} is stretching vibrations of carbon to carbon triple bond of alkyne, the band interval of 1500–1700 cm^{-1} is an indication of C=C (aromatic skeletal mode of lignin, C=O aldehyde or ketone), and can also indicate the bending vibration of adsorbed water, 1250–1000 cm^{-1} is assigned to C–O vibration of carboxylic acids, C–O–C and O–H vibration of polysaccharides, $1000–500 \text{ cm}^{-1}$ band interval is C–H and C–C bend vibration and halogenated compounds' (C–X) stretching vibration (Ahmad et al. 2017; Argun et al. 2014). Based up on the FTIR spectra each of the functional group have an affinity for adsorption.

Optimization results of different parameters
Effects of solution pH
In fact that the solution pH can affect the surface charge of the adsorbent, the degree of ionization of the different pollutants, the dissociation of functional groups on the active sites of the adsorbent as well as the structure of the dye molecule (Ai et al. 2011; Bello et al. 2017; Ghaedi et al. 2014; Mall et al. 2005). Therefore the solution pH is a master parameter during the dye adsorption process. The effect of initial pH on the MG removal was studied in the pH range of 2–12 with initial dye concentration of
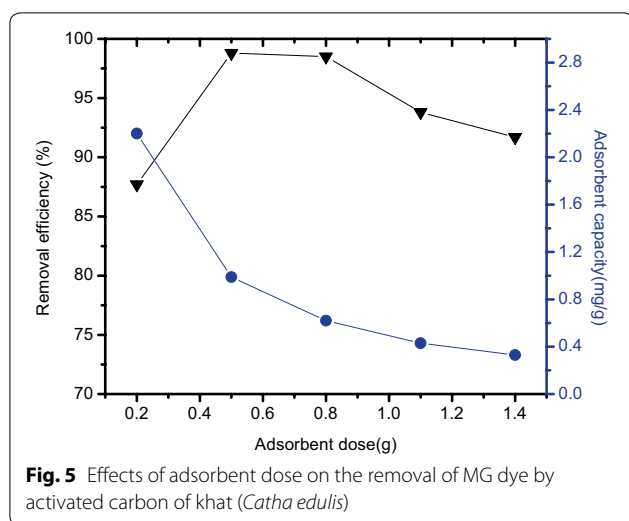
10 mg/L (50 mL) and adsorbent dose of 0.5 g and presented in Fig. 4. Removal efficiency increase with increasing solution pH until equilibrium reached. This is the fact that increasing pH leads to the formation of negative charge on the surface of adsorbent up on deprotonation reaction. This negative charge enables high removal efficiency as result of electrostatic attraction between the adsorbent and positively charged of adsorbate (MG). Whereas at lower pH, the various functional groups and reactive atom of dyes and adsorbent protonated and both get positive charge (Ai et al. 2011; Mall et al. 2005). Therefore, due to strong repulsive force between dyes and adsorbent decrease the removal percentage. As shown in Fig. 4 at acidic region (pH=2) the removal efficient is 77.5% whereas at the basic region (pH=10) is 98.8%. The removal efficiency is increase until the pH reaches to optimum beyond that slightly decrease due to competency of active site of the adsorbent.

Effects of adsorbent dose
To know the effects of the adsorbent dosage on MG removal efficiency the experiments was carried out by varying adsorbent dose from 0.2 to 1.4 g at fixed dye concentration (10 mg/L), pH=10, contact time 60 min, shaking speed 400 rpm and presented in Fig. 5. When the bio mass increased from 0.1 to 0.5 g an increase in the MG removal from 87.7 to 98.8% percentage removal was observed. This behavior could be explained considering that with adsorbent dosage increases leads to an increase on the surface; consequently, more active sites are available to bind dye from aqueous phase (Ai et al. 2011; Li et al. 2013). At masses over 0.5 g, the amount of MG slightly decreased due to the aggregation and overlapping of particles of adsorbent in the solution, consequently, a
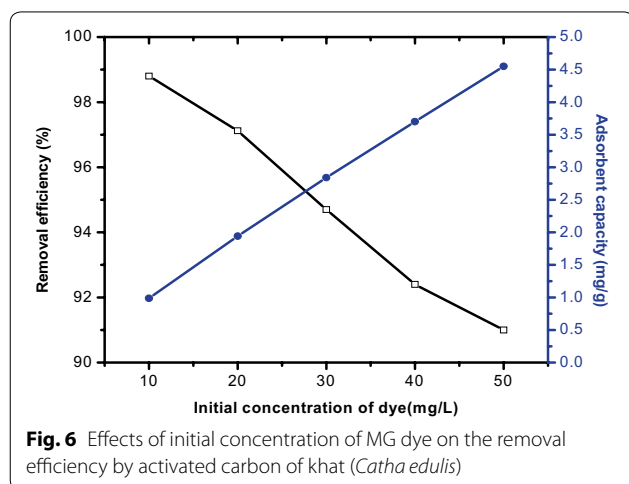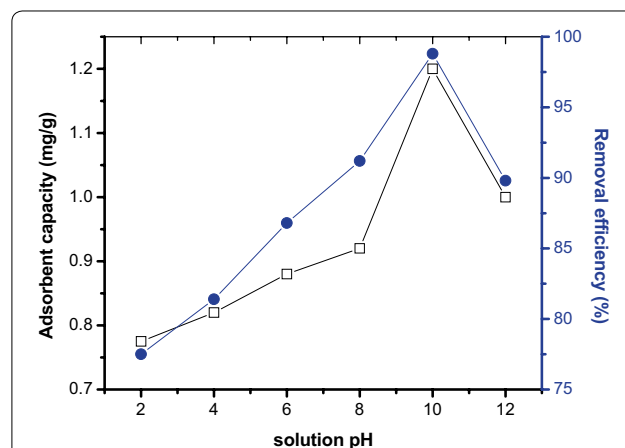

Fig. 4 Effects of solution pH on the removal of malachite green dye by activated carbon of khat (*Catha edulis*)

Abate *et al. Environ Syst Res*   (2020) 9:29

Page 7 of 13

Fig. 5 Effects of adsorbent dose on the removal of MG dye by activated carbon of khat (*Catha edulis*)

decrease in the surface for dye uptake occurs. This result is in agreement with data reported by different scholar findings (Ai et al. 2011; Lee et al. 2019). For this reason, the adsorbent mass 0.5 g was chosen for the subsequent experiments.
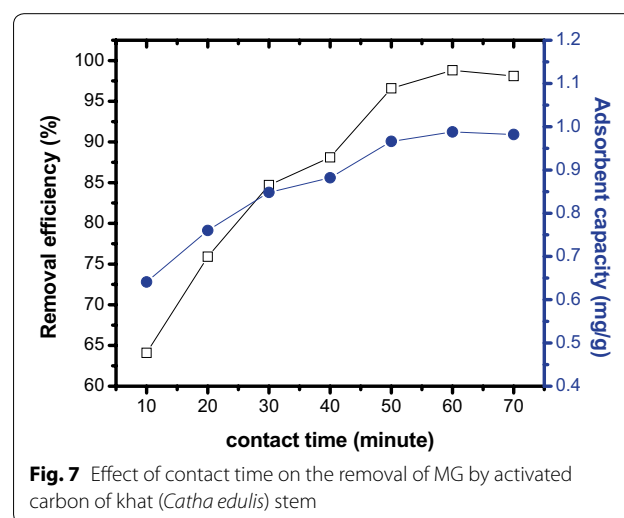
Effects of initial concentration of dye

The effect of the initial concentration of MG dye on its adsorption onto the prepared adsorbent is presented in Fig. 6. The experiment was carried out at different concentration (50 mL of 10–50 mg/L) at fixed adsorbent dose 0.5 g, pH = 10, contact time 60 min, shaking speed 400 rpm at and room temperature in batch operation mode. As shown in Fig. 6 the percentage removal of MG decrease with increasing initial concentration of dye. Since the adsorbent dose is fixed, there is a fixed number of active site as a result percentage removal decrease with increasing concentration. At low initial concentrations

of MG dye relatively high percentage sorption's were observed. As a result of the high ratio of adsorbent surface binding sites to the dye concentration, meaning that a fewer number of dye molecules were competing for the available binding sites on the adsorbent (Bello et al. 2017; Dos Reis et al. 2011; Raval et al. 2016). Although, adsorption capacity (q_e) increases with increasing initial concentration of MG dyes. As increase the initial concentration of the dye from 10 to 50 mg/L, resulted an increase in adsorption capacity (q_e) from 0.988 to 4.55 mg/g. The increase in the initial concentration of the dye enhances the interaction between the dye molecules and the surface of the adsorbent (Ai et al. 2011; Lee et al. 2019; Mondal and Kar 2018). This results can also observed with different scholars finding and reported in different literatures (Mondal and Kar 2018; Raval et al. 2016).

Effect of contact time

The effect of contact time on the MG dye adsorption by the prepared adsorbent was carried out with different contact time (10–80 min) at fixed dose 0.5 g, pH = 10, shaker speed 400 rpm and presented in Fig. 7 below. The amount adsorbed dyes first rapidly increased, and then gradually decreased until equilibrium was reached. This is perhaps due to the initial availability of maximum number of active sites which gets saturated with time. As a result, the remaining vacant surface sites are difficult to be occupied due to the formation of repulsive force between the adsorbate (MG) on the solid surface of adsorbent with adsorbate (MG) on the bulk phase (solutions) as well as the saturation of active site of the adsorbent. This trend was observed by different scholar's findings and reported in different literatures (Mondal and Kar 2018; Rahmat et al. 2016). The removal efficiency was found to be at the range of 64.1 to 98.8% when the

Fig. 6 Effects of initial concentration of MG dye on the removal efficiency by activated carbon of khat (*Catha edulis*)

Fig. 7 Effect of contact time on the removal of MG by activated carbon of khat (*Catha edulis*) stem

Abate *et al. Environ Syst Res* (2020) 9:29

Page 8 of 13

time rises from 10 to 60 min respectively. As shown in Fig. 7, the contact time required for MG to reach equilibrium was 60 min, with the removal efficiencies of 98.8%. The result showed that the prepared adsorbent has short equilibrium time which shows the adsorbent have enough number of active site for a given concentration. In fact short equilibrium time is recommendable on the view of water treatment technologies.

Kinetics studies

The kinetic profile is fundamental to study an adsorption system. Kinetic curves provides information about the adsorption rate and also, regarding to the required time to attain the equilibrium (Dos Reis et al. 2011; Ghaedi et al. 2014; Royer et al. 2009). In the present studies, adsorption kinetics was studied using the pseudo-first order (Eq. 9), pseudo second order (Eq. 10) and antiparticle diffusion model (Eq. 11) respectively (Rahmat et al. 2016; Regti et al. 2017).

$$\log (q_e - q_t) = \log q_e - k_1 t, \tag{9}$$

$$\frac{t}{q_t} = \frac{1}{K_2 q_e^2} + \frac{t}{q_e}, \tag{10}$$

$$q_t = K_{diff} t^{1/2} + C; \tag{11}$$

where q_e (mg/g) is amount adsorbed at equilibrium time; q_t (mg/g) is amount adsorbed at time, t (min); k_1 is the pseudo-first-order rate constant; k_2 is the pseudo second-order rate constant; k_{diff} (mg/g min$^{1/2}$) is the intraparticle diffusion rate constant; and C is the intercept that indicates the boundary layer thickness. The kinetic rate constant, k, and q_e for each model can be calculated by plotting graph log $(q_e - q_t)$ versus t for pseudo-first-order, t/q_t versus t for pseudo-second-order models, and q_t versus $t^{1/2}$ for intraparticle diffusion models and the graphs presented in Figs. 8, 9, and 10, respectively.

All the kinetic parameters for all kinetics models were calculated from the graph and presented in Table 3. As shown in Table 3, amount of adsorbed dyes (q_e) or q_e calculated based on pseudo-second order models very similar to experimental value as compare to pseudo 1st order and inter particle diffusion mode. Furthermore, the correlation factor (R^2) obtained calculated through pseudo-second-order models ($R^2 = 0.99684$) greater than pseudo 1st order and inter particle diffusion model. This implies that the experimental data were good agreement with pseudo second kinetics order model (Rahmat et al. 2016).
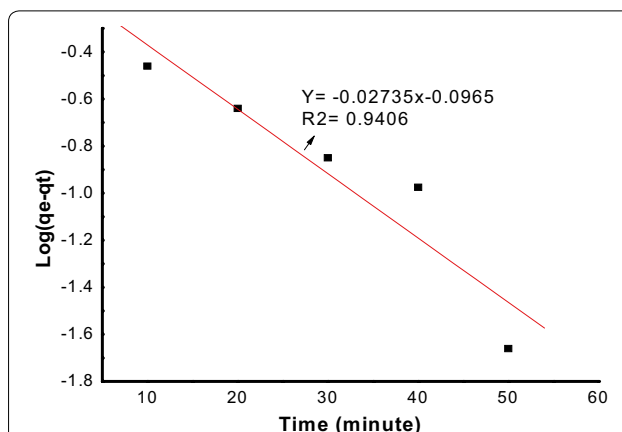
Fig. 8 pseudo first order kinetics graph at different time (10–70 min) at fixed concentration 10 mg/L, dose 0.5 g, pH = 10 and at room temperature
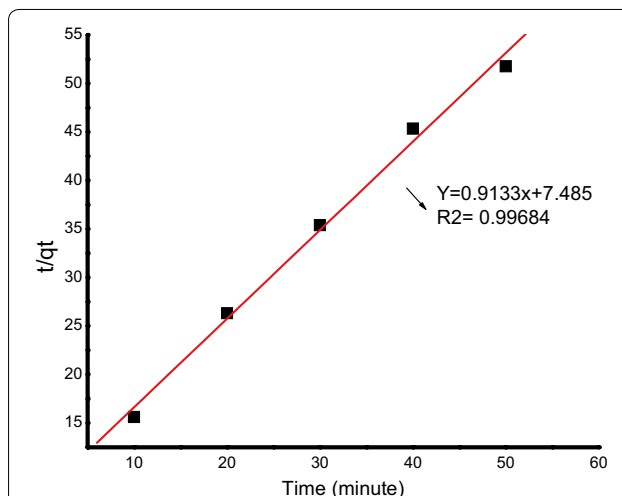

Fig. 9 Pseudo 2nd order kinetics graph at different contact time (10–70 min) at fixed concentration 50 mL of 10 mg/L, dose 0.5 g, pH = 10 and at room temperature

Equilibrium isotherm studies

Adsorption isotherms describe how the adsorbate interacts with adsorbent and provide comprehensive understanding about the nature of the interaction. Isotherms help to provide information about the optimum use of adsorbents (Raval et al. 2016). Isotherm curves are extremely relevant for adsorption purposes, since it provides information about the interaction mechanisms and maximum adsorption capacity of a determined adsorbent (Leechart et al. 2009; Regti et al. 2017). In order to

Abate *et al. Environ Syst Res*   (2020) 9:29

Page 9 of 13

Fig. 10 Interparticle diffusion model kinetics graph at different contact time (10–70 min) at fixed concentration 50 mL of 10 mg/L, dose 0.5 g and pH = 10 at room temperature
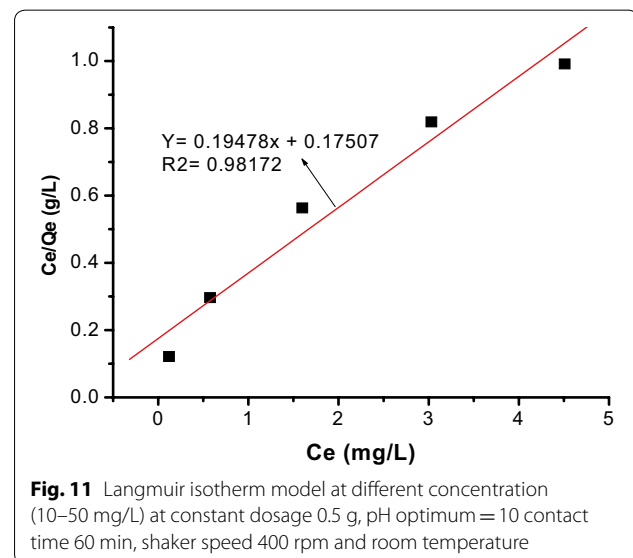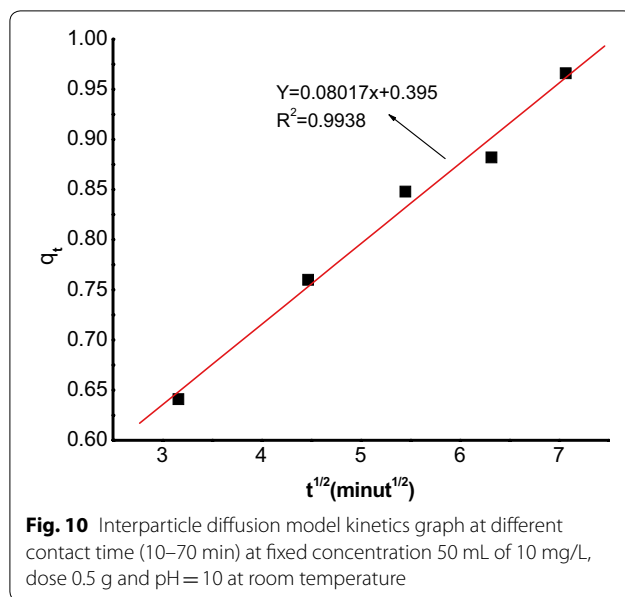
determine the best-fit bio-sorption isotherm model, the equilibrium data were analyzed by most common isotherm models such as the Langmuir and Freundlich isotherm models. They were helpful to determine the maximum adsorption capacity of adsorbate for the given adsorbent. They differ in the basic assumptions, shape of the isotherm and nature of the adsorbent surface. The Freundlich isotherm is derived by assuming a heterogeneous surface with a non-uniform distribution of heat of adsorption over the surface. Whereas in the Langmuir theory, the basic assumption is that the sorption takes place at specific homogeneous sites within the adsorbent (Bello et al. 2017; Deng et al. 2011). The mathematical expressions for those isotherms were presented in equation

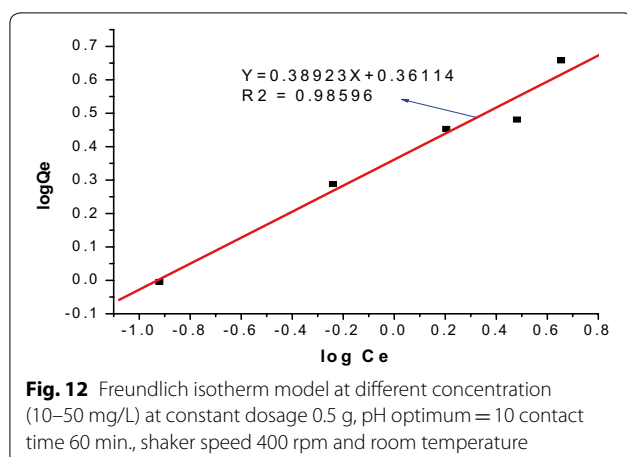$$\frac{C_e}{q_e} = \frac{1}{bq_m} + \frac{C_e}{q_m};\tag{12}$$

$$\log q_e = \log k_f + \frac{\log C_e}{n};\tag{13}$$

where C_e is the equilibrium concentration of solute (mmol/L), q_e is the amount of solute adsorbed per unit weight of adsorbent (mmol/g of adsorbate), q_m is the adsorption capacity (mmol/g), or monolayer capacity, and b is a constant (L/mmol) for Langmuir isotherm, K_f and n are empirical constants for Freundlich isotherm incorporating all parameters affecting the adsorption process such as, sorption capacity and sorption intensity respectively. The isotherm curves were drawn C_e/q_e versus C_e for Langmuir isotherm and $\log q_e$ vs. $\log c_e$ graph for Freundlich isotherm model and presented in Figs. 11, 12 respectively. The isotherm parameters such as, q_m and b for Langmuir isotherm model can be calculated from intercept and the slope of C_e/q_e versus C_e graph respectively. The value of k_f and n for Freundlich can be calculated from $\log q_e$ vs. $\log c_e$ graph. All the isotherm parameters calculated from the graph and correlation factor (R^2) for both models were presented in Table 4 below. As shown in Table 4 the collation factor for Freundlich ($R^2 = 0.98596$) close to 1 confirms Freundlich isotherm model better describes the interaction between adsorbent and adsorbate in aqueous system.

Fig. 11 Langmuir isotherm model at different concentration (10–50 mg/L) at constant dosage 0.5 g, pH optimum = 10 contact time 60 min, shaker speed 400 rpm and room temperature

Table 3 Kinetics parameters obtained from the graph

Kinetics model	q_e experimental	q_e calculated	R^2	K constant
Pseudo 1st	0.988	0.9035	0.9406	− 0.02735
Pseudo 2nd	0.988	1.09	0.99684	2.99
Interparticle diffusion model	0.988	0.395	0.9934	0.08017

Fig. 12 Freundlich isotherm model at different concentration (10–50 mg/L) at constant dosage 0.5 g, pH optimum = 10 contact time 60 min., shaker speed 400 rpm and room temperature

Table 4 Isotherm parameters calculated from the graphs

Isotherm	R^2	Estimated isotherm parameters
Langmuir	0.98172	$q_m = 5.620$ mg/g, $b = 1.02$
Freundlich	0.98596	$K_f = 2.3$ mg/g; $n = 2.57$

Table 5 Dimensionless constant separation factor (R_L) value at different initial concentration

Adsorbent	R_L values				
	Concentration (mg/L)				
	10	20	30	40	50
Activated carbon of khat (*Catha edulis*)	0.089	0.047	0.032	0.024	0.019

The Adsorption was considered as satisfactory when the Freundlich constant n took value within the range 1–10. Therefore the value of n calculated from the graph is lies on this range and Freundlich considered as satisfactory to describe adsorption.

For Langmuir type adsorption process, the efficiency of the adsorption process could be predicted by the dimensionless equilibrium parameter R_L, which is defined by the following equation in Eq. 14 (Ajenifuja et al. 2017; Li et al. 2013).
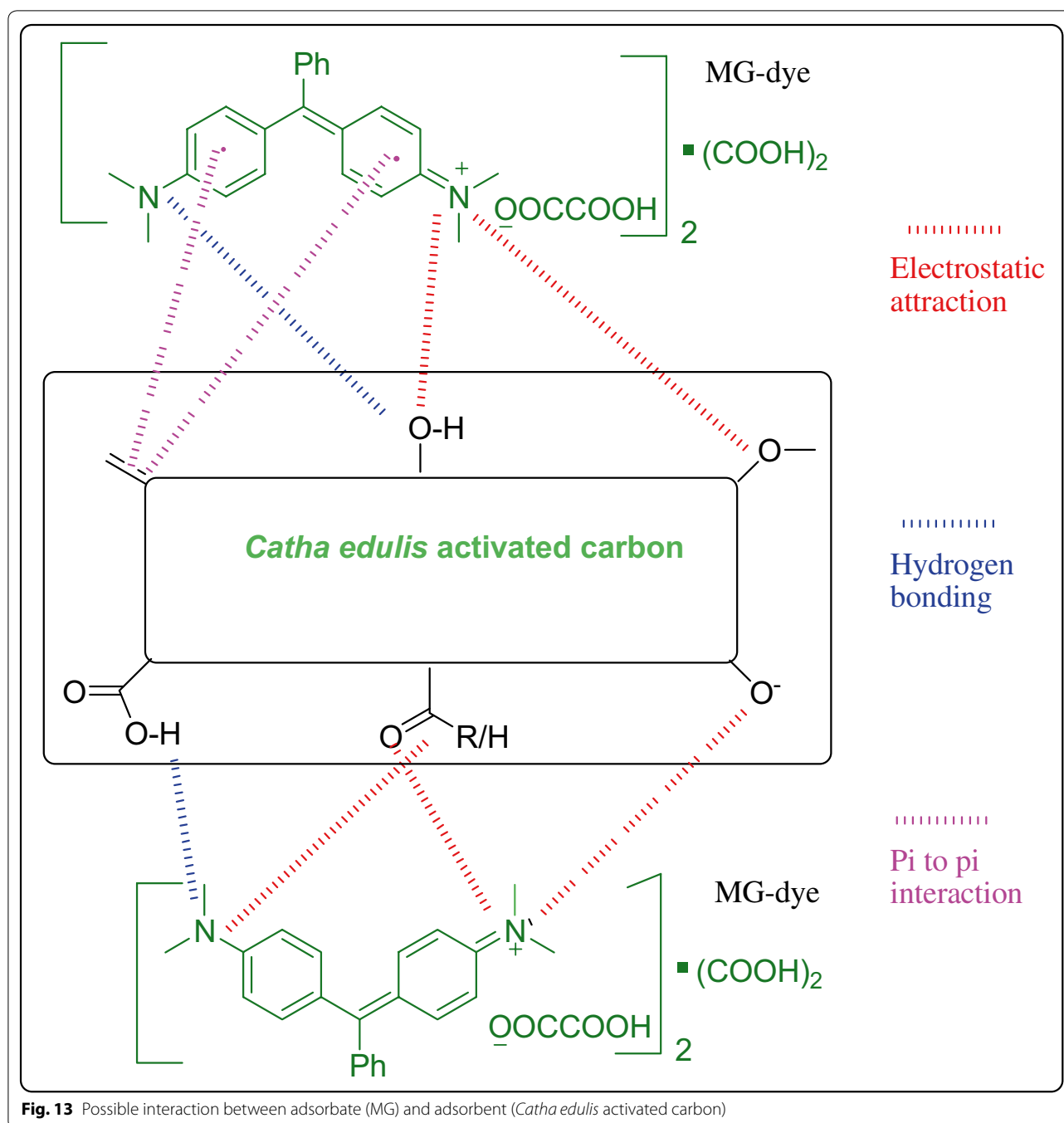
$$R_L = \frac{1}{1 + bC_0};\qquad(14)$$

where b is Langmuir constant related to the energy of adsorption (L/mg) and C_0 is initial concentration (mg/L). The calculated R_L values at different initial dye concentration were written in Table 5 below. R_L value indicates the adsorption nature to be either unfavorable if $R_L > 1$), linear if $R_L = 1$, favorable if $0 < R_L < 1$ and irreversible if $R_L = 0$ (Ajenifuja et al. 2017). For this study all the valves were lies between 0 and 1 which confirming that the adsorption of dye over the adsorbent was favorable (Ajenifuja et al. 2017).

Proposed adsorption mechanism

The adsorption of MG dye from aqueous solution by activated carbon derived from *Catha edulis* stem is strongly dependent on the various functional groups on the surface of *Catha edulis* stem such as hydroxyl, phenols, aromatics and etc. which are supported by FTIR spectral results described in Fig. 3. The surface of *Catha edulis* functional groups may be charged (negative and positive) or neutral upon protonation and deprotonation. The possible adsorption mechanism of MG dye on the surface of *Catha edulis* is summarized in Fig. 13 and the probable adsorption mechanisms between the surface functional groups of *Catha edulis* adsorbent and MG dye can be assigned to the various interactions such as electrostatic attractions, hydrogen bonding interaction and π–π interactions between the adsorbent and adsorbate (Jawad et al. 2019). Similar observation was reported for the adsorption on MG on chemically modified rice husk (Chowdhury et al. 2011). The comparison of previous study on the adsorption of MG dye by different adsorbents with the current finding is presented in Table 6.

Conclusions

The present investigation showed that activated carbon prepared from khat (*Catha edulis*) stem is an effective adsorbent for removal MG from aqueous solution. The effect of different parameters like pH, contact time, adsorbent dose and initial concentration of dye were tested. Removal of MG is pH dependent and the maximum removal was attained at basic medium pH = 10 with 98.8% percentage removal. The bio sorption MG dye at the basic medium indicated that surface charge greatly affected the dye uptake capacity. Adsorption equilibrium data tested on Langmuir and Freundlich models and equilibrium data fitted very well in Freundlich isotherm equations. The maximum MG sorption

Abate *et al. Environ Syst Res*   (2020) 9:29

Page 11 of 13

Fig. 13 Possible interaction between adsorbate (MG) and adsorbent (*Catha edulis* activated carbon)

monolayer capacity of the sorbent was found to be 5.62 mg/g. The kinetic study of MG onto activated carbon of *khat* (*Catha edulis*) stem was performed based on pseudo-first-order and pseudo-second-order model. The bio sorption kinetic was in good agreement with the pseudo-second-order model. Because of higher regression value close to 1 and adsorption capacity (q_e) calculated based on this model agreed well with the experimental q_e. In summary the present study concludes that the prepared adsorbent could be employed

Abate *et al. Environ Syst Res*   (2020) 9:29

Page 12 of 13

Table 6 Adsorption comparison of different adsorbents in MG in the literature

Adsorbent	q_m (mg/g)	pH	Isotherm	Kinetic	References
Cellulose powder	2.42	7.2	Both FIM and LIM	PSO	Sekhar et al. (2009)
Polymeric gel (C4)	4.9	8	LIM	PSO	Malana et al. (2010)
Neem saw dust	7.2	4.35	LIM	–	Khattri and Singh (2009)
Tamarind fruit shell	1.95	5	LIM	PSO	Saha (2010)
Commercial activated carbon	8.27	7	FIM	PSO	Mall et al. (2005)
Avena sativa (oat) hull	83	8	FIM	PSO	Banerjee et al. (2016)
Unsaturated polyester Ce(IV) phosphate	1.01	8	FIM	IPDM	Khan et al. (2013b)
Sepia	3.48		Both LIM and FIM	–	Figueiredo et al. (2000)
Chlorella-based biomass	18.4	–	–	PSO	Tsai and Chen (2010)
Khat edulis activated carbon	5.62	10	FIM	PSO	This study

FIM Freundlich isotherm model, *LIM* Langmuir isotherm model, *IPDM* inter particle diffusion model, *PSO* pseudo second order

as low-cost adsorbents for the removal of MG dye from wastewater.

References
Ahmad F, Daud WMAW, Ahmad MA, Radzi R (2013) The effects of acid leaching on porosity and surface functional groups of cocoa (*Theobroma cacao*)-shell based activated carbon. Chem Eng Res Des 91:1028–1038

Ahmad MA, Afandi NS, Bello OS (2017) Optimization of process variables by response surface methodology for malachite green dye removal using lime peel activated carbon. Appl Water Sci 7:717–727

Ai L, Zhang C, Liao F, Wang Y, Li M, Meng L, Jiang J (2011) Removal of methylene blue from aqueous solution with magnetite loaded multi-wall carbon nanotube: kinetic, isotherm and mechanism analysis. J Hazard Mater 198:282–290

Ajenifuja E, Ajao J, Ajayi E (2017) Adsorption isotherm studies of Cu (II) and Co (II) in high concentration aqueous solutions on photocatalytically modified diatomaceous ceramic adsorbents. Appl Water Sci 7:3793–3801

Almeida C, Debacher N, Downs A, Cottet L, Mello C (2009) Removal of methylene blue from colored effluents by adsorption on montmorillonite clay. J Colloïd Interface Sci 332:46–53

Argun ME, Güçlü D, Karatas M (2014) Adsorption of reactive blue 114 dye by using a new adsorbent: Pomelo peel. J Ind Eng Chem 20:1079–1084

Asfaram A, Fathi M, Khodadoust S, Naraki M (2014) Removal of direct red 12B by garlic peel as a cheap adsorbent: kinetics, thermodynamic and equilibrium isotherms study of removal. Spectrochim Acta A Mol Biomol Spectrosc 127:415–421

Banerjee S, Sharma GC, Gautam RK, Chattopadhyaya M, Upadhyay SN, Sharma YC (2016) Removal of Malachite green, a hazardous dye from aqueous solutions using *Avena sativa* (oat) hull as a potential adsorbent. J Mol Liq 213:162–172

Bello OS, Ahmad MA (2012) Coconut (*Cocos nucifera*) shell based activated carbon for the removal of malachite green dye from aqueous solutions. Sep Sci Technol 47:903–912

Bello OS, Adelaide OM, Hammed MA, Popoola OAM (2010) Kinetic and equilibrium studies of methylene blue removal from aqueous solution by adsorption on treated sawdust. Maced J Chem Chem Eng 29:77–85

Bello OS, Adegoke KA, Akinyunni OO (2017) Preparation and characterization of a novel adsorbent from *Moringa oleifera* leaf. Appl Water Sci 7:1295–1305

Chowdhury S, Mishra R, Saha P, Kushwaha P (2011) Adsorption thermodynamics, kinetics and isosteric heat of adsorption of malachite green onto chemically modified rice husk. Desalination 265:159–168

Deng H, Lu J, Li G, Zhang G, Wang X (2011) Adsorption of methylene blue on adsorbent materials produced from cotton stalk. Chem Eng J 172:326–334

Dos Reis LGT, Robaina NF, Pacheco WF, Cassella RJ (2011) Separation of malachite green and methyl green cationic dyes from aqueous medium by adsorption on amberlite XAD-2 and XAD-4 resins using sodium dodecylsulfate as carrier. Chem Eng J 171:532–540

Figueiredo S, Boaventura R, Loureiro J (2000) Color removal with natural adsorbents: modeling, simulation and experimental. Sep Purif Technol 20:129–141

Fito J, Said H, Feleke S, Worku A (2019) Fluoride removal from aqueous solution onto activated carbon of *Catha edulis* through the adsorption treatment technology. Environ Syst Res 8:25

Georgin J, da Silva Marques B, da Silveira Salla J, Foletto EL, Allasia D, Dotto GL (2018) Removal of procion red dye from colored effluents using $H_2SO_4^-$/HNO_3^- treated avocado shells (*Persea americana*) as adsorbent. Environ Sci Pollut Res 25:6429–6442

Ghaedi M, Tavallali H, Sharifi M, Kokhdan SN, Asghari A (2012) Preparation of low cost activated carbon from *Myrtus communis* and pomegranate and

Abate *et al. Environ Syst Res* (2020) 9:29

Page 13 of 13

their efficient application for removal of congo red from aqueous solution. Spectrochim Acta A Mol Biomol Spectrosc 86:107–114

Ghaedi M, Nasab AG, Khodadoust S, Rajabi M, Azizian S (2014) Application of activated carbon as adsorbents for efficient removal of methylene blue: kinetics and equilibrium study. J Ind Eng Chem 20:2317–2324

Ghaedi M, Hajjati S, Mahmudi Z, Tyagi I, Agarwal S, Maity A, Gupta V (2015) Modeling of competitive ultrasonic assisted removal of the dyes–methylene blue and Safranin-O using Fe_3O_4 nanoparticles. Chem Eng J 268:28–37

Giwa A, Bello I, Olajire A (2013) Removal of basic dye from aqueous solution by adsorption on melon husk in binary and ternary systems. Chem Process Eng Res 13:51–68

Gobi K, Mashitah M, Vadivelu V (2011) Adsorptive removal of methylene blue using novel adsorbent from palm oil mill effluent waste activated sludge: equilibrium, thermodynamics and kinetic studies. Chem Eng J 171:1246–1252

Gupta VK, Mohan D, Sharma S, Sharma M (2000) Removal of basic dyes (rhodamine B and methylene blue) from aqueous solutions using bagasse fly ash. Sep Sci Technol 35:2097–2113

Ho Y-S, Chiang T-H, Hsueh Y-M (2005) Removal of basic dye from aqueous solution using tree fern as a biosorbent. Process Biochem 40:119–124

Islam MA, Benhouria A, Asif M, Hameed B (2015) Methylene blue adsorption on factory-rejected tea activated carbon prepared by conjunction of hydrothermal carbonization and sodium hydroxide activation processes. J Taiwan Inst Chem Engi 52:57–64

Jawad AH, Razuan R, Appaturi JN, Wilson LD (2019) Adsorption and mechanism study for methylene blue dye removal with carbonized watermelon (*Citrullus lanatus*) rind prepared via one-step liquid phase H_2SO_4 activation. Surf Interfaces 16:76–84

Kadirvelu K, Kavipriya M, Karthika C, Radhika M, Vennilamani N, Pattabhi S (2003) Utilization of various agricultural wastes for activated carbon preparation and application for the removal of dyes and metal ions from aqueous solutions. Bioresour Technol 87:129–132

Kennedy JG (1987) The flower of paradise: the institutionalized use of the drug qat in North Yemen. Springer Science & Business Media, Berlin

Khan TA, Nazir M, Khan EA (2013a) Adsorptive removal of rhodamine B from textile wastewater using water chestnut (*Trapa natans* L.) peel: adsorption dynamics and kinetic studies. Toxicol Environ Chem 95:919–931

Khan AA, Ahmad R, Khan A, Mondal PK (2013b) Preparation of unsaturated polyester Ce (IV) phosphate by plastic waste bottles and its application for removal of Malachite green dye from water samples. Arab J Chem 6(4):361–368

Khattri S, Singh M (2009) Removal of malachite green from dye wastewater using neem sawdust by adsorption. J Hazard Mater 167:1089–1094

Kibami D, Chubaakum P, Rao K, Dipak S (2014) Preparation and characterization of activated carbon from *Fagopyrum esculentum* Moench by HNO_3 and H_3PO_4 chemical activation. Der Chemica Sinica 5:46–55

Lee LY, Gan S, Tan MSY, Lim SS, Lee XJ, Lam YF (2016) Effective removal of acid blue 113 dye using overripe *Cucumis sativus* peel as an eco-friendly biosorbent from agricultural residue. J Clean Prod 113:194–203

Lee S-L, Park J-H, Kim S-H, Kang S-W, Cho J-S, Jeon J-R, Lee Y-B, Seo D-C (2019) Sorption behavior of malachite green onto pristine lignin to evaluate the possibility as a dye adsorbent by lignin. Appl Biol Chem 62:37

Leechart P, Nakbanpote W, Thiravetyan P (2009) Application of 'waste' wood-shaving bottom ash for adsorption of azo reactive dye. J Environ Manag 90:912–920

Li Y, Du Q, Liu T, Peng X, Wang J, Sun J, Wang Y, Wu S, Wang Z, Xia Y (2013) Comparative study of methylene blue dye adsorption onto activated carbon, graphene oxide, and carbon nanotubes. Chem Eng Res Des 91:361–368

Malana MA, Ijaz S, Ashiq MN (2010) Removal of various dyes from aqueous media onto polymeric gels by adsorption process: their kinetics and thermodynamics. Desalination 263:249–257

Mall ID, Srivastava VC, Agarwal NK, Mishra IM (2005) Adsorptive removal of malachite green dye from aqueous solution by bagasse fly ash and activated carbon-kinetic study and equilibrium isotherm analyses. Colloids Surf A 264:17–28

Mezohegyi G, van der Zee FP, Font J, Fortuny A, Fabregat A (2012) Towards advanced aqueous dye removal processes: a short review on the versatile role of activated carbon. J Environ Manag 102:148–164

Mondal NK, Kar S (2018) Potentiality of banana peel for removal of congo red dye from aqueous solution: isotherm, kinetics and thermodynamics studies. Appl Water Sci 8:157

Mopoung S, Moonsri P, Palas W, Khumpai S (2015) Characterization and properties of activated carbon prepared from tamarind seeds by KOH activation for Fe (III) adsorption from aqueous solution. Sci World J. https://doi.org/10.1155/2015/451961

Munagapati VS, Yarramuthi V, Kim Y, Lee KM, Kim D-S (2018) Removal of anionic dyes (reactive black 5 and congo red) from aqueous solutions using banana peel powder as an adsorbent. Ecotoxicol Environ Saf 148:601–607

Nhung NTH, Quynh BTP, Thao PTT, Bich HN, Giang BL (2018) Pretreated fruit peels as adsorbents for removal of dyes from water, IOP Conference Series: Earth and Environmental Science. IOP Publishing, Bristol, p 012015

Nigatu A, Libsu S (2019) Studies on the effects of extracts of fresh Khat/*Catha edulis* leaves on the oxidation of Niger seed oil. J Pharm Pharmacol 7:421–428

Pathania D, Sharma S, Singh P (2017) Removal of methylene blue by adsorption onto activated carbon developed from *Ficus carica* bast. Arab J Chem 10:S1445–S1451

Rahmat NA, Ali AA, Hussain N, Muhamad MS, Kristanti RA, Hadibarata T (2016) Removal of remazol brilliant blue R from aqueous solution by adsorption using pineapple leaf powder and lime peel powder. Water Air Soil Pollut 227:105

Raval NP, Shah PU, Shah NK (2016) Nanoparticles loaded biopolymer as effective adsorbent for adsorptive removal of malachite green from aqueous solution. Water Conserv Sci Eng 1:69–81

Regti A, Laamari MR, Stiriba S-E, El Haddad M (2017) Potential use of activated carbon derived from *Persea* species under alkaline conditions for removing cationic dye from wastewaters. J Assoc Arab Univ Basic Appl Sci 24:10–18

Royer B, Cardoso NF, Lima EC, Vaghetti JC, Simon NM, Calvete T, Veses RC (2009) Applications of Brazilian pine-fruit shell in natural and carbonized forms as adsorbents to removal of methylene blue from aqueous solutions—kinetic and equilibrium study. J Hazard Mater 164:1213–1222

Safarik I, Horska K, Svobodova B, Safarikova M (2012) Magnetically modified spent coffee grounds for dyes removal. Eur Food Res Technol 234:345–350

Saha P (2010) Assessment on the removal of methylene blue dye using tamarind fruit shell as biosorbent. Water Air Soil Pollut 213:287–299

Sekhar CP, Kalidhasan S, Rajesh V, Rajesh N (2009) Bio-polymer adsorbent for the removal of malachite green from aqueous solution. Chemosphere 77:842–847

Sharma P, Kaur R, Baskar C, Chung W-J (2010) Removal of methylene blue from aqueous waste using rice husk and rice husk ash. Desalination 259:249–257

Silveira MB, Pavan FA, Gelos NF, Lima EC, Dias SL (2014) *Punica granatum* shell preparation, characterization, and use for crystal violet removal from aqueous solution. CLEAN Soil Air Water 42:939–946

Temesgen F, Gabbiye N, Sahu O (2018) Biosorption of reactive red dye (RRD) on activated surface of banana and orange peels: economical alternative for textile effluent. Surf Interfaces 12:151–159

Tsai WT, Chen HR (2010) Removal of malachite green from aqueous solution using low-cost chlorella-based biomass. J Hazard Mater 175:844–849

Yakout AA, Shaker MA (2016) Dodecyl sulphate functionalized magnetic graphene oxide nanosorbent for the investigation of fast and efficient removal of aqueous malachite green. J Taiwan Inst Chem Eng 63:81–88

Zhang L, Zhang H, Guo W, Tian Y (2014) Removal of malachite green and crystal violet cationic dyes from aqueous solution using activated sintering process red mud. Appl Clay Sci 93:85–93

Publisher's Note